J Appl Physiol 119: 1337–1346, 2015.
First published September 24, 2015; doi:10.1152/japplphysiol.00255.2015.

The proportion of common synaptic input to motor neurons increases with an increase in net excitatory input

Anna Margherita Castronovo,[1,2] Francesco Negro,[1] Silvia Conforto,[2] and Dario Farina[1]

[1]*Department of Neurorehabilitation Engineering, Bernstein Focus Neurotechnology, Bernstein Center for Computational Neuroscience, University Medical Center Göttingen, Georg-August University, Göttingen, Germany; and* [2]*BioLab, Biomedical Engineering Laboratory, Department of Engineering, University Roma TRE, Rome, Italy*

Submitted 25 March 2015; accepted in final form 22 September 2015

Castronovo AM, Negro F, Conforto S, Farina D. The proportion of common synaptic input to motor neurons increases with an increase in net excitatory input. *J Appl Physiol* 119: 1337–1346, 2015. First published September 24, 2015; doi:10.1152/japplphysiol.00255.2015.—α-Motor neurons receive synaptic inputs from spinal and supraspinal centers that comprise components either common to the motor neuron pool or independent. The input shared by motor neurons—common input—determines force control. The aim of the study was to investigate the changes in the strength of common synaptic input delivered to motor neurons with changes in force and with fatigue, two conditions that underlie an increase in the net excitatory drive to the motor neurons. High-density surface electromyogram (EMG) signals were recorded from the tibialis anterior muscle during contractions at 20, 50, and 75% of the maximal voluntary contraction force (in 3 sessions separated by at least 2 days), all sustained until task failure. EMG signal decomposition identified the activity of a total of 1,245 motor units. The coherence values between cumulative motor unit spike trains increased with increasing force, especially for low frequencies. This increase in coherence was not observed when comparing two subsets of motor units having different recruitment thresholds, but detected at the same force level. Moreover, the coherence values for frequencies <5 Hz increased at task failure with respect to the beginning of the contractions for all force levels. In conclusion, the results indicated that the relative strength of common synaptic input to motor neurons increases with respect to independent input when the net excitatory drive to motor neurons increases as a consequence of a change in force and fatigue.

common synaptic input; motor neuron; net excitation; task failure; coherence; motor neuron spike trains

MOTOR NEURONS RECEIVE both common and independent synaptic inputs from the motor cortex, brain stem, and spinal circuitries (32). These inputs are integrated to generate trains of action potentials. The ensemble of motor neuron activations is referred to as the neural drive to the muscle (4). The presence of common synaptic input to motor neurons determines a certain degree of correlation in the output trains of discharge times (48) which depends on the strength of the common synaptic input with respect to the independent synaptic noise (15, 39). The investigation of the correlation between the spike trains discharged by a pool of motor neurons makes it possible to infer the connectivity of the pool with the spinal and cortical circuitries (38). The synchronization in discharge times has been attributed to excitatory and inhibitory postsynaptic potentials arriving at the motor neuron from branch axons of the presynaptic neurons (29), to the activity of interneuronal circuits or peripheral afferents (50), or to the presence of oscillators within the motor cortex or brain stem (49).

Even if the origin of common input to motor neurons is not fully understood, it has been recently postulated that the common synaptic input to motor neurons represents the effective neural drive delivered to muscles (20). Indeed, the cumulative output of the motor neurons in the pool corresponds to an averaging process that filters out independent components while transmitting common components (20). Therefore, the common input is the only input component that influences the control of force (19). The presence of common input and, as a consequence, of correlated activity of motor neurons is thus necessary for force control. The neural drive to muscle is a noisy version of the common input where the noise is progressively attenuated for greater numbers of recruited motor neurons (20). A simple model that represents common and independent input to motor neurons is described in the APPENDIX.

The degree of correlation between motor unit discharge times induced by common input can be investigated either in the time or in the frequency domain (with coherence analysis) (45, 24). The correlation at frequencies <3 Hz is associated with the so called "common drive" (16), while the α band (5–12 Hz) is related to the production of slow movements (53) and physiological tremor (13), the β band (15–30 Hz) to the corticospinal drive, and the low γ band (30–60 Hz) to the activity of the motor cortex (10). For a given number of discharge times used for the estimation of coherence between groups of motor units, the coherence magnitude is associated to the relative proportion of common synaptic input with respect to the independent inputs to motor neurons (39).

The presence of a synchronous activity between motor neurons plays an important role in the understanding of how the nervous system controls muscle forces. On the one hand, delivering common synaptic input to motor neurons allows the central nervous system to regulate force efficiently (23, 3, 47, 37). On the other hand, a too high level of synchronization due to common input may disrupt the motor performance (2, 27, 55).

In this study, we compared the proportion of common input with respect to independent input using coherence analysis between groups of motor units during sustained isometric contractions of the tibialis anterior muscle at different net excitation levels. Given the fact that the common input may be originated by multiple sources, we will refer to common input as the total amount of synaptic input that is shared across the motor neurons in the pool. The change in the excitation level to the muscle was obtained either by changing the force produced by the muscle or by sustaining a single force level until task

Address for reprint requests and other correspondence: D. Farina, Institute for Neurorehabilitation Systems Bernstein Focus Neurotechnology Göttingen, Bernstein Center for Computational Neuroscience, Universitätsmedizin Göttingen, Georg-August Universität, von Siebold-Str. 6, 37075 Göttingen, Germany (e-mail: dario.farina@bccn.uni-goettingen.de).

8750-7587/15 Copyright © 2015 the American Physiological Society

Downloaded from http://jap.physiology.org/ by 10.220.33.5 on November 28, 2016

failure. Because the number of shared projections to the motor neuron pool presumably increases with an increase in excitation drive, we hypothesized that the relative strength of common input would increase with both increasing force and during the sustained isometric task.

Preliminary results of this study have been reported in abstract form (11, 12).

MATERIALS AND METHODS

Participants. Ten healthy men (age: 31.6 ± 3.4 yr) volunteered for the study. None of the participants reported a previous history of knee or ankle pathology or surgery. An informed written consent, approved by the Ethical Committee of the Universitätmedizin Göttingen (approval no. 04/12/11), was signed by all the subjects before participating in the experiments.

Experimental protocol. The participants performed sustained isometric contractions of the tibialis anterior muscle until task failure at 20, 50, and 75% of the maximal voluntary contraction (MVC) force. Task failure was defined as the time instant when the subject exerted a force 10% MVC below the target force for an interval of time of 2 s. The three task failure tasks at the three force levels were performed on separate days (2 days minimum separation) and were randomized in order. At the beginning of each experimental session, the participants were asked to progressively increase the ankle dorsiflexion force to the maximum force level and to maintain it for 3 s. This task was repeated three times. The highest force value among the three trials was taken as reference value for the MVC. The measure of the MVC was repeated after the end of the isometric contraction to verify the occurrence of fatigue. The participants were provided with a visual feedback of force during the execution of each trial.

Force and electromyogram recordings. The participants were seated in an upright position, with the right leg fully extended and with the foot restrained in a force transducer (Biodex Multi Joint System 3, Biodex Medical systems, Shirley, NY). The angle of the ankle was ~20° with respect to the neutral position (0°). The leg was fastened to the isokinetic device by means of Velcro straps to avoid altering the position of the ankle throughout the tasks. The force signals were sampled at 5,000 samples/s. Surface electromyographic (EMG) signals were recorded from the tibialis anterior muscle by using a semidisposable adhesive matrix with 64 channels (8-mm interelectrode distance; OT Bioelettronica, Torino, Italy), mounted on the surface of the muscle with an adhesive foam. The skin was shaved, lightly abraded with abrasive paste (Meditec-Every, Parma, Italy), and cleansed before placing the electrodes. The EMG signals were recorded in differential mode, amplified (EMG-USB, LISiN–OT Bioelettronica, Torino, Italy), sampled at 2,048 samples/s, and digitized via a 12 bit A/D converter. The data recorded were analyzed off-line by using custom written codes developed in MATLAB (Mathworks, Natick, MA). The first 10 s after the beginning of the task and the last 10 s before task failure were analyzed.

Force data analysis. Force traces were low-pass filtered with a fourth-order Butterworth filter with a cutoff frequency of 20 Hz. The data, sampled at 5,000 Hz, were downsampled to 2,048 Hz and then synchronized with the EMG traces. Force steadiness was quantified by using the coefficient of variation of force, defined as the percent ratio between the standard deviation and the mean force.

Surface EMG analysis. Surface EMG signals were band-pass filtered with a 20–500 Hz Butterworth filter. EMG amplitude was estimated as the root mean square value of the central signal of the grid. The multichannel surface EMG signals were then decomposed into motor unit spike trains by using the convolution kernel compensation (CKC) decomposition framework (25). This algorithm relies on blind source separation and guarantees high accuracy in the identification of motor unit discharges for the tibialis anterior muscle even at high contraction levels (26). Spike trains of single motor units were then obtained with a sampling frequency of 1,000 samples/s. The instantaneous discharge rate of each of the decomposed motor units was smoothed by using a 1-s Hanning window and then averaged across the pool to characterize the global discharge. The variability of the interspike interval was estimated by calculating the coefficient of variation of the unfiltered motor unit spike trains for each force level and both conditions. This parameter has been computed as the percentage of the ratio between the standard deviation and the average values of firing times in a moving window of 1 s and by using an overlap of 90%.

The degree of correlation between spike trains was calculated in the frequency domain by means of coherence analysis on the unfiltered composite spike trains (summation of individual spike trains) (38, 39). The analysis was performed on two groups of five motor unit spike trains each, summed to obtain a cumulative spike train per group (39). It has been previously demonstrated that the correlation between cumulative trains of discharges of motor neurons monotonically increases with the number of motor unit spike trains used for its calculation (39, 20). The function representing the coherence value as a function of the number of motor neuron spike trains is therefore a monotonically increasing function. In particular, the rate of the increase depends on the proportion of common input with respect to the independent one, with a faster increase when more common input is present. Thus for a similar number of motor units used for the estimation, differences in coherence represent differences in the strength of common input. When coherence is computed between pairs of motor units, the estimated correlation strength tends to be weaker than the one computed between the summed spike trains of two populations of motor units. The estimated correlation tends to increase with the number of motor units up to a saturation value. This is a consequence of the summation process as well since it tends to cancel the noncorrelated components of the synaptic input so that only correlated signal components remain in the output (39, 44, 42). In this study, we analyzed the coherence values across conditions assuring the same number of motor unit spike trains in each group. This number was five and was chosen as a tradeoff between the minimum number of motor units identified at the highest contraction level and a sufficient number of units to reach a high sensitivity in the comparisons with respect to the classic approach (i.e., coherence between pairs of motor units; see Ref. 44 for details). The coherence obtained in this way was then compared across force levels and between fatigue stages, with the final aim of providing a single measure representative of the entire data set. The magnitude squared coherence values were estimated by using the mscohere function of MATLAB, with a 1-s Hanning window and an overlap of 90%. The obtained values were then averaged ("pooled") across the total number of combinations (i.e., 100).

The coherence values (C) were converted to Fisher's values (FZ), and then an intrinsic bias was removed from each profile.

$$FZ = \arctanh\left(\sqrt{C}\right) \quad (1)$$

The Fisher's transformation acts as a normalization procedure for the variance of the coherence estimates (8) and it has been used in several other studies (36, 34, 14, 43). The bias was empirically determined as the maximum value of the coherence profile for frequencies higher than 100 Hz since no significant correlated activity exists in this range (4). The coherence profiles were averaged across subjects and analyzed in the frequency bands 1–5 , 5–10 , 10–30 , and 30–80 Hz. Since overlapped segments were used to compute coherence to decrease the bias and the variance of the estimation, we decided not to normalize the Fisher's value, as instead it is recommended by Amjad and colleagues (1). In fact, when overlapped windows are used, the statistics of the magnitude squared profiles is unknown (7).

For the sustained tasks, since the motor units decomposed at the beginning and at the end of the tasks were presumably different because of progressive recruitment, we also repeated the estimation of

Downloaded from http://jap.physiology.org/ by 10.220.33.5 on November 28, 2016

the coherence restricted only to those motor units that could be identified both at the beginning and at the end of the contractions. This analysis was performed on a reduced number of subjects (three) at only one contraction level (50% MVC) because of the difficulty in matching individual motor units over the full duration of task failure tasks. We decomposed the entire trials by dividing the overall duration in epochs of 10 s. The motor units that were identified in the first epoch were then matched with the ones in the next epoch by using spike-triggered averaging and 2D correlation analysis. Only the motor units that were firing in the first 10 s and were still firing in the last 10 s of the trial were considered for coherence analysis. The results in this subset of data allowed us to exclude the changes in coherence that were observed over time during the sustained contractions (see RESULTS) due to differences in recruitment thresholds of the identified motor units.

The analysis of common units could not be performed across different force levels since the recordings for each level were performed on separate days with subjects exhibiting different values of maximal force. However, to exclude an effect of the recruitment threshold in the comparisons (17), we assessed differences in coherence between groups of motor units with different thresholds within the same contraction level. For this purpose, we first identified the motor units firing during the 50% MVC initial ramp contraction, and then we estimated their recruitment thresholds. Subsequently, these motor units were matched with the ones identified in the first 10 s of the sustained tasks at both 20 and 50% MVC. This analysis was performed on three subjects for each contraction level. The recruitment threshold range identified for each pool of motor neurons was then divided into two groups with respect to the median value of the interval. Values lower than the median were used to identify low-threshold motor units and, in the same way, values higher than the median characterized the high-threshold motor units. Then, for each subject and for each group of motor units, the pooled coherence was computed according to Amjad and colleagues (1). These values were then converted to Fisher's values; an inherent bias was also removed from each coherence profile by subtracting the maximal coherence value for frequencies higher than 100 Hz (4).

To evaluate changes in the estimated pooled coherence between low- and high-threshold motor neurons, we also computed the standard difference of the coherence test at each frequency as follows:

$$\Delta Z = FZ_2 - FZ_1 \quad (2)$$

Since also in this case the same number of overlapped segments were used to calculate coherence in both conditions, we decided not to normalize the difference of Fisher's z scores. To identify frequency bands with consistent changes in coherence due to the recruitment threshold, the ΔZ profiles again underwent Stouffer's method; in this way, a positive value of ΔZ indicated greater coherence estimations for the high-threshold motor units while negative values indicated the opposite.

Statistics. All the extracted variables underwent a Kolmogorov-Smirnov test to check the assumption of being normally distributed. Since most of them were not distributed according to a standard normal distribution, nonparametric statistical tests were used. In fact, it has been reported that a nonparametric approach performs better in the case of multiple comparisons and in the control of type I errors (34). First of all, a Friedman's test was performed by using a data structure of $10 \times 3 \times 2$ [by using 10 subjects as repetitions, 3 force levels, and 2 conditions (beginning vs. fatigue)]. Because of the restriction of Friedman's test, it was not possible to evaluate the mutual interactions a priori. Thus nonparametric statistical tests were computed on significant residuals. A Wilcoxon rank sum test was applied to evaluate the changes introduced by the sustained contraction (beginning vs. task failure) for the same variables (coefficient of variation of force, firing rate, coefficient of variation of interspike interval, EMG root mean square, and coherence). A Kruskal-Wallis one-way analysis of variance (with force level as a factor) was instead applied to the residuals to characterize the influence of an increased contraction force on force steadiness, EMG amplitude level, discharge frequency and its variability, and coherence between motor unit spike trains. All differences were considered significant for P values less than 0.05. For the analysis conducted on the groups of motor neurons with different recruitment thresholds within the same force contraction, the Z-transformed coherence values of the ΔZ profiles higher than ± 1.65 in each of the frequency bands of interest were considered as statistically influenced by the recruitment threshold of the motor neurons. All differences were considered significant for P values less than 0.05. For the analysis conducted on the groups of motor neurons with different recruitment thresholds within the same force contraction, the Z-transformed coherence values of the ΔZ profiles higher than ± 1.65 in each of the frequency bands of interest were considered as statistically influenced by the recruitment threshold of the motor neurons.

RESULTS

We decomposed 1,245 motor units in total, with an average number of 21 ± 7 motor units per contraction force per subject. An example of the motor unit discharge trains obtained from the decomposition of 30 s of EMG signal at the beginning and at the end of a 20% MVC contraction is shown in Fig. 1.

Figure 2 shows the results for the coefficient of variation of force, the EMG root mean square, the discharge frequency, and its variability when force increased. The coefficient of variation of force increased with force ($P = 0.002$), from $0.7 \pm 3.3\%$ (20% MVC) to $0.8 \pm 2.7\%$ (50% MVC) to $1.6 \pm 1.9\%$ (75% MVC) (Fig. 2*A*). The EMG amplitude also increased with the exerted force ($P = 0.0001$) by $88.7 \pm 47.4\%$ from 20% to 50% MVC, by $230 \pm 104.6\%$ from 20% to 75% MVC, and by $84.7 \pm 47.7\%$ from 50% to 75% MVC (Fig. 2*B*). The average discharge rates of the identified motor units were 11 ± 0.8 pps (20% MVC), 14.7 ± 1.9 pps (50% MVC), and 15.8 ± 2.6 pps (75% MVC) (Fig. 2*C*). Also, the variability of the interspike interval increased with contraction level ($P = 0.001$). In particular, it varied from $18.01 \pm 8.3\%$ (20% MVC) to $25.03 \pm 11.1\%$ (50% MVC) to $34.03 \pm 11.7\%$ (75% MVC) (Fig. 2*D*).

Immediately after task failure, the maximal voluntary force decreased significantly for all contraction levels (by $21.2 \pm 12.6\%$ at 20% MVC, $P = 0.001$; $22.7 \pm 6.2\%$ at 50% MVC, $P = 0.00001$; $11 \pm 5.6\%$ at 75% MVC, $P = 0.003$). Figure 3 shows the coefficient of variation of force, the EMG-RMS, the discharge frequency, and the coefficient of variation of the interspike interval at the beginning of the sustained contractions and at task failure. In particular, at task failure, the coefficient of variation of force increased with respect to the beginning of the contraction for the force levels of 20 and 50% MVC ($0.7 \pm 0.2\%$ vs. $3.3 \pm 1.9\%$ at 20% MVC; $0.8 \pm 0.3\%$ vs. $2.7 \pm 1.7\%$ at 50% MVC), but not for 75% MVC ($1.6 \pm 0.7\%$ vs. $1.9 \pm 1.3\%$) (Fig. 3*A*). The surface EMG amplitude also increased at the end with respect to the beginning of the contractions only for 20 and 50% MVC (50 ± 20 μV vs. 80 ± 40 μV for 20% MVC; 90 ± 20 μV vs. 150 ± 50 μV for 50% MVC) and not for 75% MVC (150 ± 50 μV vs. 200 ± 80 μV) (Fig. 3*B*). The increase in surface EMG amplitude at task failure was not associated with the global discharge rate since discharge rate did not change significantly during the fatiguing contractions (Fig. 3*C*). Instead, the variability of the discharge timings changed with fatigue only at 20 and 50% MVC force levels ($18.01 \pm 8.3\%$ vs. $26.4 \pm 12.6\%$, $P = 0.01$, for

Downloaded from http://jap.physiology.org/ by 10.220.33.5 on November 28, 2016

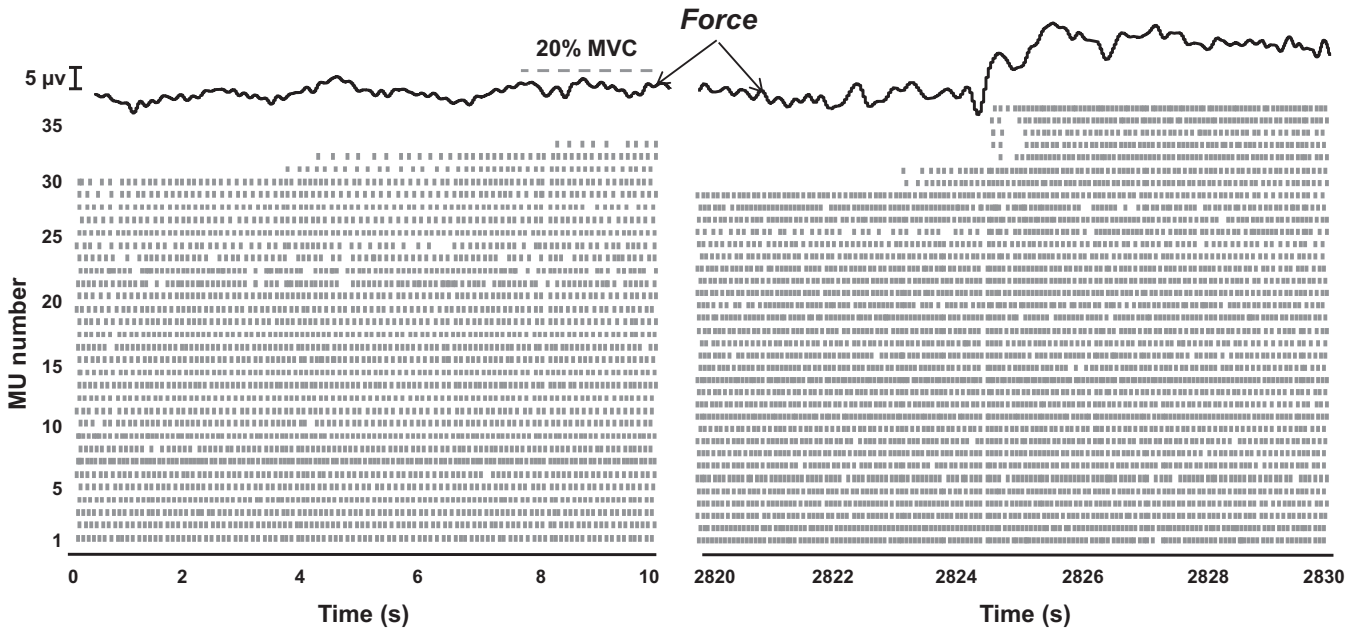

Fig. 1. Example of motor unit discharge times identified from the decomposition of 10 s of electromyogram (EMG) signals at the beginning (*left*) and at the end (*right*) of a 20% maximal voluntary contraction (MVC) contraction. The bold black line on the top represents the force signal in the corresponding time intervals considered for the decomposition (units, μV). At the beginning of the contraction (*left*) there is a substantial recruitment of additional motor units (MU) over time, which continues until the approaching of task failure (*right*). As can be noticed from the figure at *right*, the number of motor units decomposed is higher than the beginning and the recruitment phenomenon is still present.

20% MVC and 25.03 ± 11.1 vs. 38.2 ± 10.3, $P = 0.005$, for 50% MVC) but it did not show any significant changes for the 75% MVC (34.03 ± 11.7 vs. 35.5 ± 10.7, $P = 0.67$). These changes are shown in Fig. 3*D*.

Common synaptic input. The magnitude of the coherence differed for the three force levels. Figure 4, *A* and *B*, show the coherence and the z-coherence profiles, respectively, pooled across all subjects for each of the three force targets. The coherence values increased with force only for δ and α bands (Fig. 4*C*, δ band $P = 0.03$; α band $P = 0.04$). To exclude the possibility that this result was due to differences in recruitment thresholds between the compared motor unit populations, we made an additional analysis of motor units with different thresholds but analyzed at the same force level. Despite that it

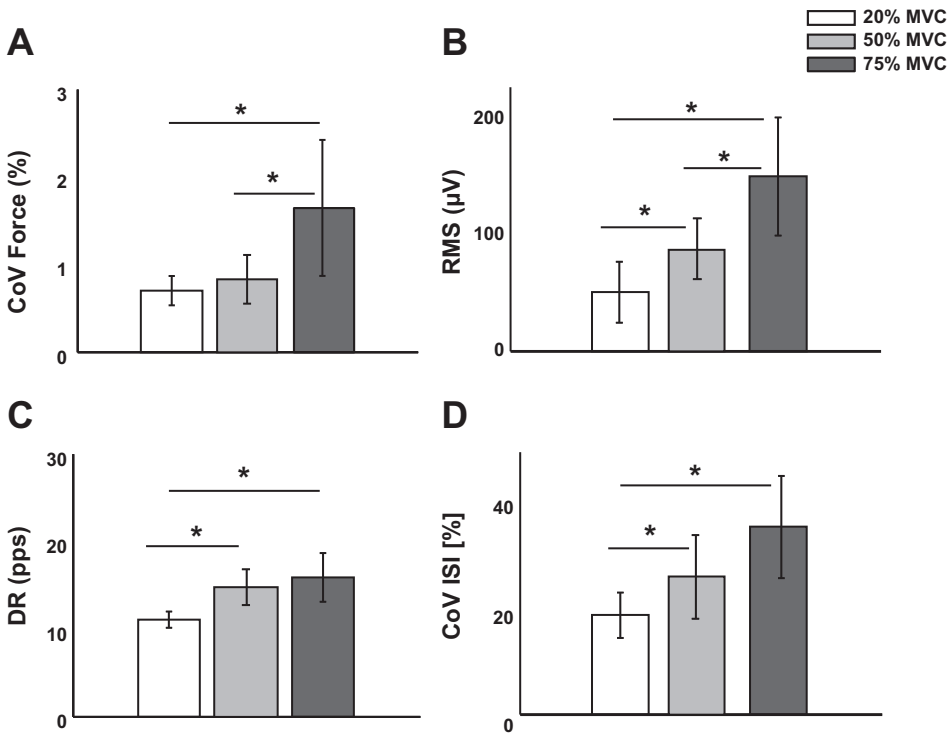

Fig. 2. Coefficient of variation (CoV) of force expressed as a percentage (*A*); EMG root mean square (RMS, μV) (*B*); motor unit discharge rate (DR) for the three contraction forces tested [pulses per second (pps)] (*C*); and coefficient of variation of the interspike interval (ISI) expressed as a percentage (%) (*D*). Data shown are relative to the first 10 s of the contraction for each force level. As can be noticed, the force oscillations increase with the contraction level and so does the EMG activity level due to the higher number of motor units recruited. The discharge characteristics and the variability of the discharge change as well with the force level. *$P < 0.05$.

Downloaded from http://jap.physiology.org/ by 10.220.33.5 on November 28, 2016

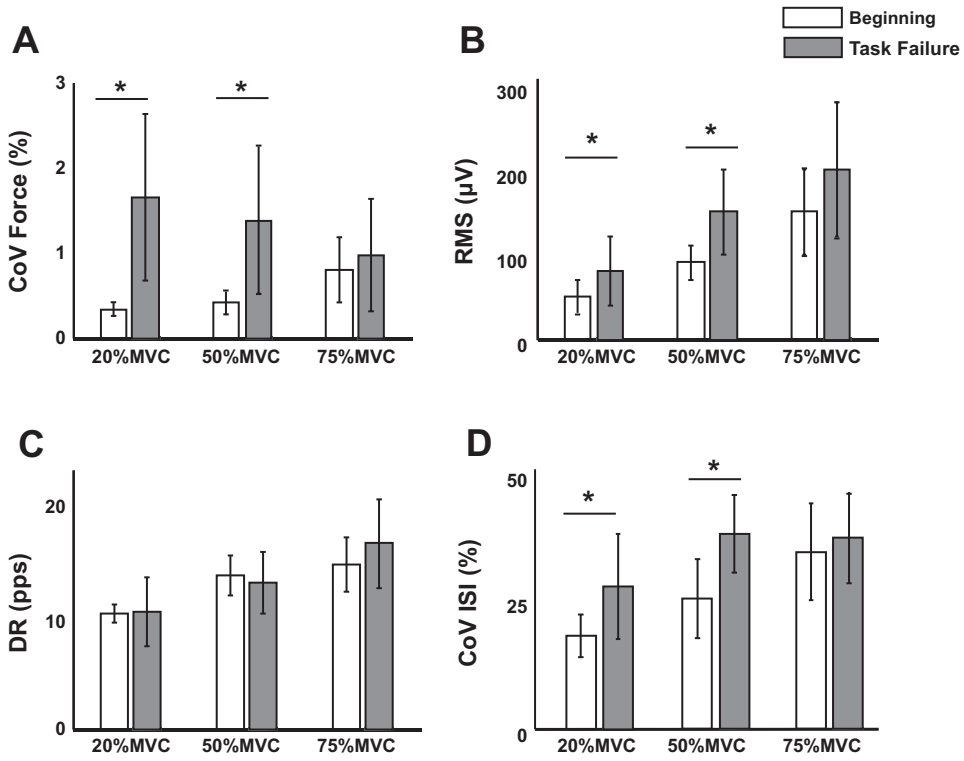

Fig. 3. Coefficient of variation of force expressed as a percentage (*A*); EMG-RMS (*B*); discharge frequency (*C*); and coefficient of variation of the interspike interval expressed as a percentage compared among the first 10 s (beginning) and the last 10 s (task failure) of all contraction levels (*D*). The coefficient of variation of force increases at task failure for all force levels but the highest one (75% MVC), and the same behavior is replicated by the EMG activity level and by the variability of firing rate. The discharge characteristics, instead, do not show any change for all contractions. $*P < 0.05$.

has been recently shown that the synchronization of the motor neuron firings depends on the recruitment threshold (17), we did not find any statistical difference in coherence values at different force intensities due to recruitment threshold. Furthermore, the overall number of action potentials discharged by the decomposed motor units at different forces for all subjects did not change significantly (from 261 ± 70 at 20% MVC to 306 ± 129 at 50% MVC to 289 ± 174 at 75% MVC, $P = 0.86$).

The coherence between motor unit spike trains was significantly greater at the end with respect to the beginning of the fatiguing task, mainly in the common drive bandwidth. Moreover, the influence of conditions (beginning vs. task failure) on force levels was reported to be significant only in the δ and α bands ($P = 0.0001$ and $P = 0.02$, respectively). The coherence profiles at the beginning and at the end of the task are depicted in Fig. 5, *A–C*. Analysis on residuals showed that the coherence values in the δ range increased at task failure with respect to the beginning of the contraction for all force levels, whereas in the α-band this occurred only for contractions at 20% MVC (Fig. 5).

We also calculated the correlation between the coefficient of variation of force and the coherence for the frequency bands of interest. As expected, the δ and α ranges showed a positive correlation with the force variability ($R^2 = 0.3$ and $R^2 = 0.2$, respectively), while poor or no correlation at all was reported for the β and γ ranges.

The coherence was also computed for the motor unit spike trains obtained from 7 ± 2 motor units per subject that were tracked along the entire duration of a 50% MVC contraction of three subjects.

Figure 6*A* shows the coherence profiles obtained for each subject from the same motor units for the first and the last 10 s of a 50% MVC contraction. Figure 6*B* shows the coherence profiles obtained by averaging over the three subjects. In agreement with the results obtained with the entire pool of motor units, the coherence values computed on this subgroup of units and averaged across subjects increased in the δ (from 0.2 ± 0.1 to 0.4 ± 0.1) and α (from 0.12 ± 0.1 to 0.3 ± 0.1) bands and in the β and γ ranges (from 0.01 ± 0.01 to 0.12 ± 0.1 and from 0.01 ± 0.0 to 0.04 ± 0.03), respectively. This test indicated that the increase in coherence with fatigue cannot be explained only by additional recruitment of motor units with higher thresholds during the fatiguing tasks. The behavior was consistent for all the three subjects.

DISCUSSION

This study analyzed the common synaptic input to the motor neuron pool of the tibialis anterior muscle during sustained contractions at different force intensities and with fatigue. The main observation was an increase in coherence values between motor unit spike trains when increasing force and when fatigue occurred. This observation indicates a relative increase in the proportion of common synaptic input to motor neurons with respect to the independent input when the net excitatory input to the motor neurons increases.

It has been previously shown that when the excitatory drive to motor neurons increases, the synaptic noise also increases with a concurrent increase in the conductance of the motor neurons and in the fluctuations in their membrane potentials (6). The present study, however, shows that, despite a potential increase in synaptic noise, the relative proportion of common input increases more rapidly than the independent one with the net excitation. Therefore, the influence of synaptic noise decreases with net excitation.

Downloaded from http://jap.physiology.org/ by 10.220.33.5 on November 28, 2016

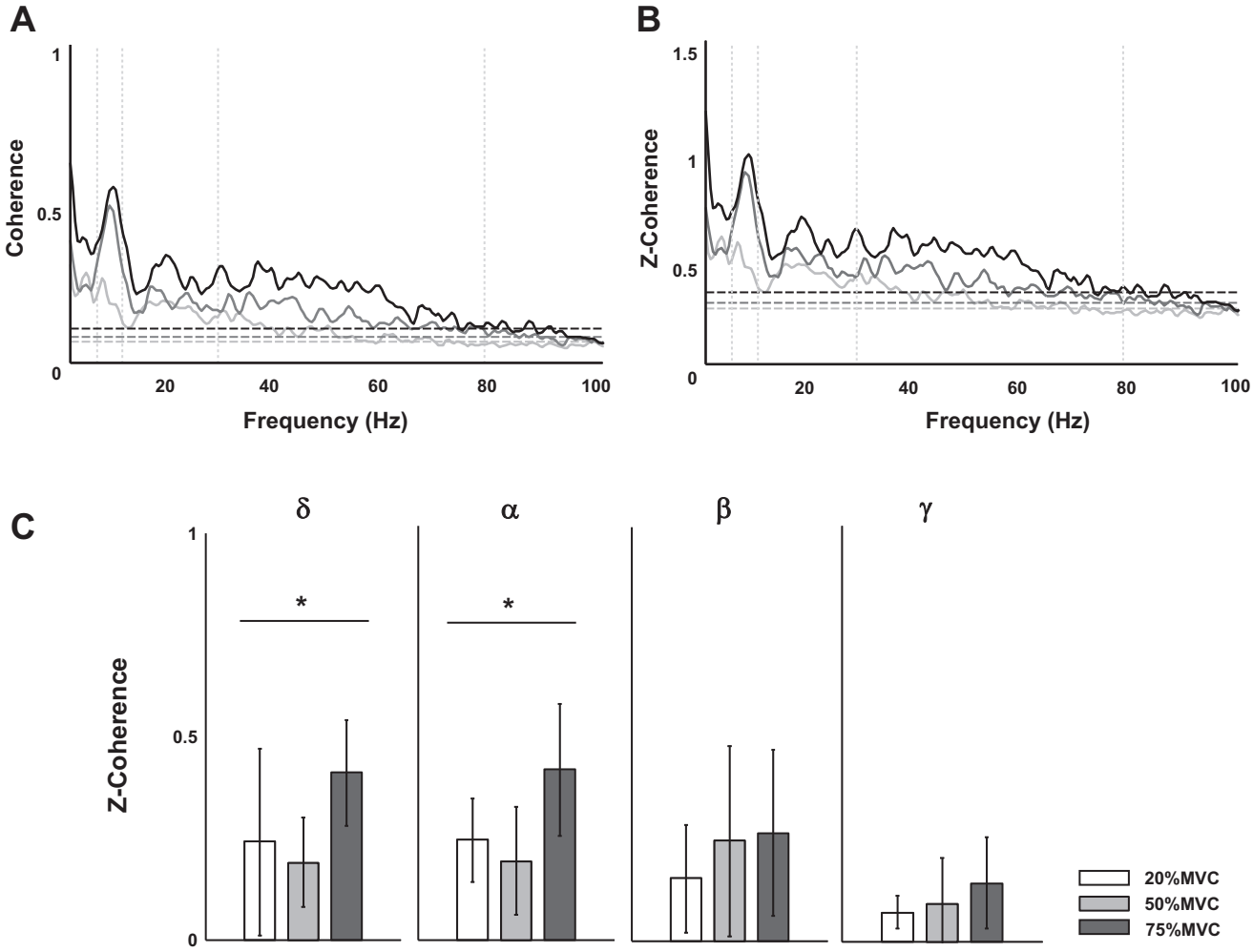

Fig. 4. *A*: coherence profiles depicted for all contraction levels with the respective confidence levels (horizontal dashed lines). *B*: z-coherence profiles are depicted for all contraction levels with the respective confidence level (horizontal dashed lines). The vertical dotted lines highlight the four frequency regions analyzed: δ-band (1–5 Hz); α-band (5–10 Hz), β-band (10–30 Hz), and γ-band (30–80 Hz). Profiles are shown for frequencies up to 100 Hz. As can be noticed, the profiles after 80 Hz are mostly below the confidence levels. *C*: histogram representation of the z score coherence values averaged across subjects are reported for the three contraction levels and the analyzed frequency bands. Only the δ and α band show significant changes because of the increased contraction levels. $*P < 0.05$.

The coherence between motor unit spike trains increased with an increase in force, as a result of stronger input oscillations generated by both branched axons or correlated activity coming from anatomically separated pathways. In particular, coherence values in the low-frequency range (δ-band) changed across all conditions. This frequency band is believed to reflect the effective control signal to the motor neuron pool because it contains information on the frequency range of the force signal (33, 40, 20, 22), and thus the increase of coherence in this range may have functional consequences. These results are supported also by the observation of a positive correlation between the force variability and the coherence in the δ and α bands, but not for higher frequencies. These results are due to the fact that the force produced by the muscle is approximately the neural drive to the muscle filtered by the average twitch (low pass) of the active motor units (5). For the intrinsic properties of this filter, the oscillations above 10 Hz are filtered out, and thus the force signal is reflected in the low-frequency band of the synaptic input. Moreover, the coherence in the low-frequency range increased also at task failure for all force levels. When task failure approaches, the excitatory drive to the motor neurons increases to maintain the required force. This mechanism is confirmed by the increase in the EMG activity, estimated as the root mean square, as a sign of progressive recruitment of newer motor units (21). Coherence between motor unit spike trains increased at task failure not only when assessing different motor units at the beginning and the end of the contraction, but also when analyzing the same motor units throughout the whole task. This indicates that the coherence level is not associated with differences in recruitment threshold, as also confirmed when comparing motor units with different thresholds at the same force level.

The increase in the common oscillations in the low-frequency band of the neural drive to muscle at task failure was reported for all force intensities. This phenomenon may be explained by an increased level of activity of the active pathways (supraspinal and spinal) and the recruitment of new pathways when task failure occurs. Such mechanism is responsible for the increased variance of the common synaptic noise. It has been reported that the populations of motor neurons

Downloaded from http://jap.physiology.org/ by 10.220.33.5 on November 28, 2016

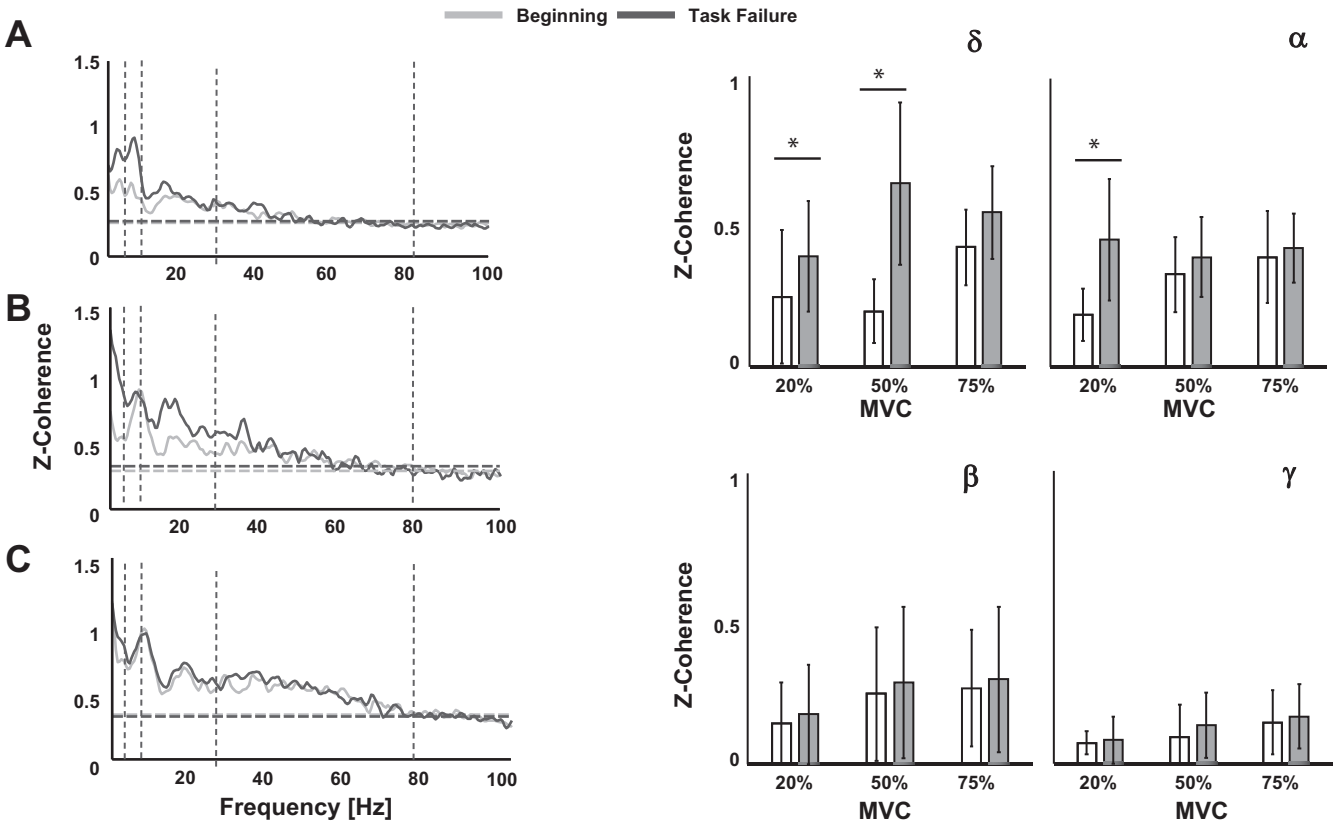

Fig. 5. *Left*: z-coherence spectra averaged across all subjects shown for both conditions (beginning vs. task failure) and starting from the top for 20% MVC (*A*), 50% MVC (*B*), and 75% MVC (*C*). *Right*: histogram representation of the z-coherence values averaged across subjects after bias removal for all contraction level and for the frequency bands: δ (1–5 Hz), α (5–10 Hz), β (10–30 Hz), and γ (30–80 Hz). Significance levels (*$P < 0.05$) are shown for the pairs: beginning vs. task failure.

projecting in the tibialis anterior muscle and in general in the distal muscles of both upper and lower limbs show strong latency facilitation when exposed to surface anodal stimulation or transcranial magnetic stimulation (31, 9, 41). This means that these motor neurons are more readily excitable by stimulation than others innervating, for example, proximal muscles (9). This has been attributed to a different distribution of the number of projections of the fast corticospinal pathways with monosynaptic projections of motor neurons. The increased coherence with increased neural excitation may thus be due to an enhancement of the supraspinal and spinal projections into the spinal cord.

We also reported a tendency toward the increase in the magnitude of coherence for frequencies higher than the common drive band, up to 80 Hz, although these changes were not significant mainly due to the high variability exhibited from the coherence profiles in these ranges. It has been demonstrated, both in monkeys and humans, that during sustained contractions from moderate to maximal levels, the coherence in the β band reproduces an effective interaction between cortical and spinal pathways (30), and that the coherence contributions tend to shift from the β to γ range with increasing force (10, 36). In our study, we did not identify a clear shift of the coherence values toward higher frequencies, but mostly an enhancement of the corticospinal coupling with the increase in force. On the contrary, we did not report any significant changes of coherence in the β and γ bands due to task failure. The changes in the interaction between cortical and spinal structures due to fatigue have not been clarified yet. β Band coherence has been shown to be dependent on the muscle and the task. Some studies reported an enhancement of coherence in the β and γ bandwidths with fatigue in the tibialis anterior (52) and hand muscles (28), while Yang et al. noticed a weakening of the cortico-muscular coupling in similar conditions for the elbow flexor muscles (54). Semmler and colleagues (51) also reported no fatigue-related changes in the β and γ band during eccentric exercises of the upper limb performed up to endurance. They attributed their observation to the weaker contribution of the corticospinal pathway to proximal muscles compared with distal. These results were confirmed in the first dorsal interosseous muscle where an increase in the α and β band was found during fatiguing contractions (35). In the present study, a tendency toward an increase in coherence at task failure was observed in the β and γ range, but it was not significant. This tendency may be explained by an increased excitation to the motor neurons through the cortico-spinal pathway.

The concept that the common part of the synaptic input increases at different force levels is further reinforced by the observed increase in the variability of force output, the higher discharge frequencies, and the greater EMG amplitude which are translated into an increase of the input delivered to motor neurons that are synchronized at a presynaptic level (47). Moreover, the variability in the interspike interval increased for all force levels, except for the 75% MVC. This may be due

Downloaded from http://jap.physiology.org/ by 10.220.33.5 on November 28, 2016

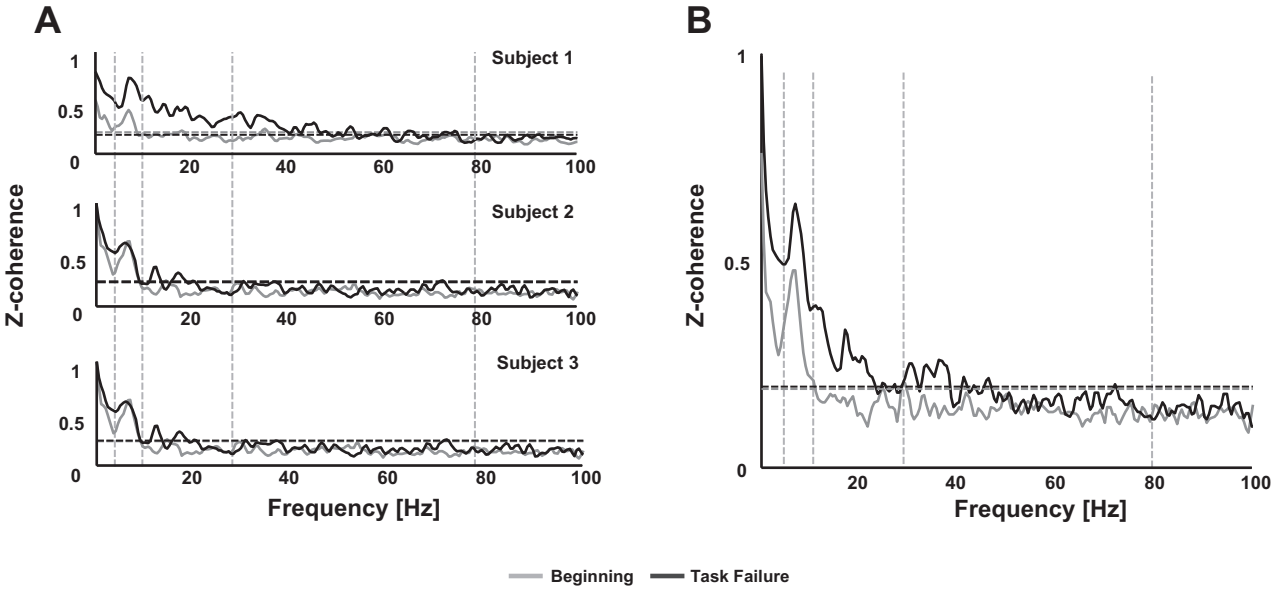

Fig. 6. *A*: coherence profiles relative to three different subjects computed over composite spike trains of motor units active from the beginning until the end of a 50% MVC contraction. The grey line represents the coherence in the first 10 s of the contraction, while the black one is the coherence computed on the same motor units but in the last 10 s of the task before the force dropped down. The same motor units were assured by spike-triggered averaging and 2D correlation analysis over epochs of 10 s. *B*: coherence profiles averaged across all three subjects and compared between the first and the last 10 s of the task. As it can be noticed, the coherence spectra are different in all the analyzed frequency bands and with significant contributions with respect to the confidence levels, ensuring that the higher values at the end of the contraction are not due to the recruitment of higher threshold motor units. Horizontal dashed lines represents the confidence level for each profile. Vertical dotted lines represents the frequency bands of interest. All coherence profiles are shown for frequencies up to 100 Hz to show the nonexistence of significant contributions for frequencies higher than 80 Hz.

to the fact that motor unit recruitment ended around 75% MVC. In fact, the newly recruited motor units are characterized by a larger variability in the discharge which influences the overall variability of the pool. The behavior exhibited by the firing variability is, however, not surprising since the spike trains tend to reflect the periodic increases in excitation (46). Thus the larger the oscillation of the input are, the greater the firing variability will be. These results are in agreement with those previously reported in the literature. Specifically, the variability of the interspike interval depends on the total variance of the synaptic input. Thus the observed increase of the coefficient of variation of the discharge timings may indicate an increase in both the common and independent inputs. Nonetheless, a concomitant increase in the magnitude of the coherence function calculated from multiple motor neuron spike trains is in agreement with an increase of common synaptic input mainly (see APPENDIX). It has also to be considered that an increase in net excitatory input to the motor neurons may have influenced the motor neuron gain. However, a potential change in gain would likely influence the transmission of both the common and the independent input and would therefore not change the main conclusions of the study. Also, the increase in common synaptic input in the low-frequency band (mostly δ) is directly associated with the control of force (see APPENDIX). In fact, it has been demonstrated that the main determinant of force variability is the total common input that is delivered to motor neurons (20). The main factor challenging the accuracy of force production is indeed the variance of the common synaptic input (18). Further investigations are needed to understand if the same findings are consistent for proximal muscles (41) or for the muscles in the upper limb (9).

In conclusion, we reported an increase in coherence between cumulative trains of motor unit discharges both with force and with fatigue, i.e., with an increase of the net excitation. We interpret these results as an increase of the proportion of the common component of the synaptic input to motor neurons with respect to the independent one.

APPENDIX

Common Synaptic Input to Motor Neurons

A pool of N motor neurons receive a total synaptic current $v_i(t)$, for $i = 1{:}N$, which can be assimilated to the sum of two terms: $s(t)$ and $n_i(t)$. The first term does not depend on the motor neuron, with the exception of a constant offset, whereas $n_i(t)$ is a signal independent across motor neurons. With these notations:

$$v_i(t) = s(t) + n_i(t) \qquad i = 1, 2, \ldots N-1, N \qquad (A1)$$

$s(t)$ can be expressed as the sum of a constant value μ_i (offset) that represents the mean of the synaptic current to the i-th motor neuron, and a time-dependent term, $s^c(t)$, which is identical, apart from a constant scaling factor, for all motor neurons. *Equation A1* can thus be rewritten as:

$$v_i(t) = \mu_i + \alpha_i \cdot s^C(t) + n_i(t) \qquad i = 1:N \qquad (A2)$$

When the synaptic currents in *Eq. A2* reach the pool of N motor neurons, they determine a cumulative output which is the sum of the outputs due to the common and independent inputs, in addition to the nonlinear components. In the sum that generates the neural drive to the muscle, however, the only consistent output, common to all motor neurons, is the one due to the common input, whereas the other output components will be filtered out by the summation process since they are different for each neuron. In these conditions, the only term that determines force variations over time (and thus force control) is the

Downloaded from http://jap.physiology.org/ by 10.220.33.5 on November 28, 2016

common time-varying term $s^c(t)$. Thus following a time-varying trajectory of force is possible by modulating the common input signal $s^c(t)$.

ACKNOWLEDGMENTS

The authors thank Prof. Roger M. Enoka at the University of Colorado Boulder for the precious suggestions he gave to improve the manuscript.

GRANTS

This work has been financially supported by the European Research Council Advanced Grant DEMOVE (No. 267888).

DISCLOSURES

No conflicts of interest, financial or otherwise, are declared by the author(s).

AUTHOR CONTRIBUTIONS

A.M.C., F.N., and D.F. conceived and designed research; A.M.C. performed experiments; A.M.C. and F.N. analyzed data; A.M.C., F.N., S.C., and D.F. interpreted results of experiments; A.M.C. prepared figures; A.M.C., F.N., and D.F. drafted manuscript; A.M.C., F.N., S.C., and D.F. edited and revised manuscript; A.M.C., F.N., S.C., and D.F. approved final version of manuscript.

REFERENCES

1. **Amjad AM, Halliday DM, Rosenberg JR, Conway BA.** An extended difference of coherence test for comparing and combining several independent coherence estimates: theory and application to the study of motor units and physiological tremor. *J Neurosci Methods* 73: 69–79, 1997.
2. **Baker JR, Davey NJ, Ellaway PH, Fridland C.** Short-term synchrony of motor unit discharge during weak isometric contraction in Parkinson's disease. *Brain* 115: 137–154, 1992.
3. **Baker SN, Kilner JM, Pinches EM, Lemon RN.** The role of synchrony and oscillations in the motor output. *Exp Brain Res* 128: 109–117, 1999.
4. **Baker SN, Pinches EM, Lemon RN.** Synchronization in monkey motor cortex during a precision grip task. II. Effect of oscillatory activity on corticospinal output. *J Neurol* 89: 1941–1953, 2003.
5. **Baldissera F, Cavallari P, Cerri G.** Motoneuronal pre-compensation for the low-pass filter characteristics of muscle. *A* quantitative appraisal in cat muscle units. *J Physiol* 511: 611–627, 1998.
6. **Berg RW, Alaburda A, Hounsgaard J.** Balanced inhibition and excitation drive spike activity in spinal half-centers. *Science* 315: 390–393, 2007.
7. **Bortel R, Sovka P.** Approximation of statistical distribution of magnitude squared coherence estimated with segment overlapping. *Signal Process* 87: 1100–1117, 2007.
8. **Brillinger DR.** *Time series: data analysis and theory*. Philadelphia, PA: SIAM, 1981.
9. **Brouwer B, Ashby P.** Corticospinal projections to lower limb motoneurons in man. *Exp Brain Res* 89: 649–654, 1992.
10. **Brown P, Salenius S, Rothwell JC, Hari R.** Cortical correlate of the Piper rhythm in humans. *J Neurophysiol* 80: 2911–2917, 1998.
11. **Castronovo AM, Negro F, D'Alessio T, Farina D.** Coherence between motor unit spike trains increases during sustained fatiguing contractions of the tibialis anterior muscle. *Program No*. 746.02/UU1. 2013 Neuroscience Meeting Planner. San Diego, CA: Soc for Neurosci, 2013.
12. **Castronovo AM, Negro F, Farina D.** The relative strength of common synaptic input to motorneurons increases with force. Bernstein Conference, Göttingen, Germany, 2014. doi:10.12751/nncn.bc2014.0142.
13. **Conway BA, Farme SF, Halliday DM, Rosenberg JR.** On the relation between motor-unit discharge and physiological tremor. In: *Alpha and Gamma Motor Systems*, edited by Taylor A, Gladden MH, and Durbaba R. Boston, MA: Springer US, 1995, p. 596–598.
14. **Danna-Dos Santos A, Poston B, Jesunathadas M, Bobich LR, Hamm, TM, Santello M.** Influence of fatigue on hand muscle coordination and EMG-EMG coherence during three-digit grasping. *J Neurophysiol* 104: 3576–3587, 2010.
15. **De La Rocha J, Doiron B, Shea-Brown E, Josić K, Reyes A.** Correlation between neural spike trains increases with firing rate. *Nature* 448: 802–806, 2007.
16. **De Luca CJ, LeFever RS, McCue MP, Xenakis AP.** Control scheme governing concurrently active human motor units during voluntary contractions. *J Physiol* 329: 129–142, 1982.
17. **Defreitas JM, Beck TW, Ye X, Stock MS.** Synchronization of low- and high-threshold motor units. *Muscle Nerve* 49: 575–583, 2014.
18. **Dideriksen JL, Negro F, Enoka RM, Farina D.** Motor unit recruitment strategies and muscle properties determine the influence of synaptic noise on force steadiness. *J Neurophysiol* 107: 3357–3369, 2012.
19. **Farina D, Negro F.** Common synaptic input to motor neurons, motor unit synchronization and force control. *Exerc Sport Sci Rev* 43: 23–33, 2015.
20. **Farina D, Negro F, Dideriksen J.** The effective neural drive to muscles is the common synaptic input to motor neurons. *J Physiol* 593: 3427–3441, 2014.
21. **Farina D, Merletti R, Enoka RM.** The extraction of neural strategies from the surface EMG: an update. *J Appl Physiol* 117: 1215–1230, 2014.
22. **Farina D, Negro F, Gizzi L, Falla D.** Low-frequency oscillations of the neural drive to the muscle are increased with experimental muscle pain. *J Neurophysiol* 107: 958–965, 2012.
23. **Farmer SF.** Rhythmicity, synchronization and binding in human and primate motor systems. *J Physiol* 509: 3–14, 1998.
24. **Farmer SF, Bremner FD, Halliday DM, Rosenberg JR, Stephens JA.** The frequency content of common synaptic inputs to motoneurones studied during voluntary isometric contraction in man. *J Physiol* 470: 127–155, 1993.
25. **Holobar A, Zazula D.** Multichannel blind source separation using convolution kernel compensation. *Signal Process IEEE Trans* 55: 4487–4496, 2007.
26. **Holobar A, Minetto M, Farina D.** Accurate identification of motor unit discharge patterns from high-density surface EMG and validation with a novel signal-based performance metric. *J Neural Eng* 11: 016008, 2014.
27. **Holtermann A, Grönlund C, Karlsson JS, Roeleveld K.** Motor unit synchronization during fatigue: described with a novel sEMG method based on large motor unit samples. *J Electromyogr Kinesiol* 19: 232–241, 2009.
28. **Kattla S, Lowery MM.** Fatigue related changes in electromyographic coherence between synergistic hand muscles. *Exp Brain Res* 202: 89–99, 2010.
29. **Kirkwood P, Sears T.** The synaptic connexions to intercostal motoneurones as revealed by the average common excitation potential. *J Physiol* 275: 103–134, 1978.
30. **Kristeva R, Patino L, Omlor W.** Beta-range cortical motor spectral power and corticomuscular coherence as a mechanism for effective corticospinal interaction during steady-state motor output. *Neuroimage* 36: 785–792, 2007.
31. **Lemon R.** Descending pathways in motor control. *Annu Rev Neurosci* 31: 195–218, 2008.
32. **Lemon RN, Mantel GW, Muir RB.** Corticospinal facilitation of hand muscles during voluntary movement in the conscious monkey. *J Physiol* 381: 497–527, 1986.
33. **Mannard A, Stein RB.** Determination of the frequency response of isometric soleus muscle in the cat using random nerve stimulation. *J Physiol* 229: 275–296, 1973.
34. **Maris E, Oostenveld R.** Nonparametric statistical testing of EEG-and MEG-data. *J Neurosci Methods* 164: 177–190, 2007.
35. **McManus LM, Hu X, Rymer WZ, Suresh NL, Lowery MM.** Fatigue-related alterations to intra-muscular coherence. *7th Int IEEE/EMBS Neural Eng Conf* 2015, p. 902–905
36. **Mima T, Simpkins N, Oluwatimilehin T, Hallett M.** Force level modulates human cortical oscillatory activities. *Neurosci Lett* 275: 77–80, 1999.
37. **Murthy VN, Fetz EE.** Effects of input synchrony on the firing rate of a three-conductance cortical neuron model. *Neural Comput* 6: 1111–1126, 1994.
38. **Negro F, Farina D.** Linear transmission of cortical oscillations to the neural drive to muscles is mediated by common projections to population of motoneurons in humans. *J Physiol* 589: 629–637, 2011.
39. **Negro F, Farina D.** Factors influencing the estimates of correlation between motor unit activities in humans. *PLoS One* 7: e44894, 2012.
40. **Negro F, Holobar A, Farina D.** Fluctuations in isometric muscle force can be described by one linear projection of low-frequency components of motor unit discharge rates. *J Physiol* 587: 5925–5938, 2009.
41. **Palmer E, Ashby P.** Corticospinal projections to upper limb motoneurones in humans. *J Physiol* 448: 397–412, 1992.

Downloaded from http://jap.physiology.org/ by 10.220.33.5 on November 28, 2016

42. **Perkel DH, Gerstein GL, Moore GP.** Neuronal spike trains and stochastic point processes: II. Simultaneous spike trains. *Biophys J* 7: 419–440, 1967.
43. **Poston B, Danna-Dos Santos A, Jesunathadas M, Hamm TM, Santello M.** Force-independent distribution of correlated neural inputs to hand muscles during three-digit grasping. *J Neurophysiol* 104: 1141–1154, 2010.
44. **Rosenbaum R, Trousdale J, Josić K.** The effects of pooling on spike train correlations. *Front Neurosci* 5: 58, 2011.
45. **Rosenberg JR, Amjad AM, Breeze P, Brillinger DR, Halliday DM.** The Fourier approach to the identification of functional coupling between neuronal spike trains. *Prog Biophys Mol Biol* 53: 1–31, 1989.
46. **Salinas E, Sejnowski TJ.** Impact of correlated synaptic input on output firing rate and variability in simple neuronal models. *J Neurosci* 20: 6193–6209, 2000.
47. **Schmied A, Descarreaux M.** Influence of contraction strength on single motor unit synchronous activity. *Clin Neurophysiol* 121: 1624–1632, 2010.
48. **Sears TA, Stagg D.** Short-term synchronization of intercostal motoneurone activity. *J Physiol* 263: 357–381, 1976.
49. **Semmler JG.** Motor unit synchronization and neuromuscular performance. *Exerc Sport Sci Rev* 30: 8–14, 2001.
50. **Semmler JG, Nordstrom MA, Wallace CJ.** Relationship between motor unit short-term synchronization and common drive in human first dorsal interosseous muscle. *Brain Res* 767: 314–320, 1997.
51. **Semmler JG, Ebert SA, Amarasena J.** Eccentric muscle damage increases intermuscular coherence during a fatiguing isometric contraction. *Acta Physiol (Oxf)* 208: 362–375, 2013.
52. **Ushiyama J, Katsu M, Masakado Y, Kimura A, Liu M, Ushiba J.** Muscle fatigue-induced enhancement of corticomuscular coherence following sustained submaximal isometric contraction of the tibialis anterior muscle. *J Appl Physiol* 110: 1233–1240, 2011.
53. **Vallbo AB, Wessberg J.** Organization of motor output in slow finger movements in man. *J Physiol* 469: 673–691, 1993.
54. **Yang Q, Fang Y, Sun C, Siemionow V, Ranganathan VK, Khoshknabi D, Davis MP, Walsh D, Sahgal V, Yue GH.** Weakening of functional corticomuscular coupling during muscle fatigue. *Brain Res* 1250: 101–112, 2009.
55. **Yao W, Fuglevand RJ, Enoka RM.** Motor-unit synchronization increases EMG amplitude and decreases force steadiness of simulated contractions. *J Neurophysiol* 83: 441–452, 2009.

Downloaded from http://jap.physiology.org/ by 10.220.33.5 on November 28, 2016